FULL PAPER

Dalton
www.rsc.org/dalton

Zinc(II) complexes with intramolecular amide oxygen coordination as models of metalloamidases

Juan C. Mareque Rivas,* Emiliano Salvagni, Ravi Prabaharan, Rafael Torres Martín de Rosales and Simon Parsons

School of Chemistry, The University of Edinburgh, Joseph Black Building, King's Buildings, West Mains Road, Edinburgh, UK EH9 3JJ. E-mail: Juan.mareque@ed.ac.uk.

Received 1st October 2003, Accepted 4th November 2003
First published as an Advance Article on the web 18th November 2003

Polydentate ligands (6-R^1-2-pyridylmethyl)–R^2 (R^1 = NHCO^{t}Bu, R^2 = bis(2-pyridylmethyl)amine **L**^{1}, bis(2-(methylthio)ethyl)amine **L**^{2} and $N(CH_2CH_2)_2S$ **L**^{3}) form mononuclear zinc(II) complexes with intramolecular amide oxygen coordination and a range of coordination environments. Thus, the reaction of $Zn(ClO_4)_2\cdot 6H_2O$ with **L**$^{1–3}$ in acetonitrile affords $[(L)Zn](ClO_4)_2$ (L = **L**^{1}, **1**; **L**^{2}, **2**) and $[(L^3)Zn(H_2O)(NCCH_3)](ClO_4)_2$ **3**. The simultaneous amide/water binding in **3** resembles the motif that has been proposed to be involved in the double substrate/nucleophile Lewis acidic activation and positioning mechanism of amide bond hydrolysis in metallopeptidases. X-ray diffraction, ^{1}H and ^{13}C NMR and IR data suggests that the strength of amide oxygen coordination follows the trend **1** > **2** > **3**. **L**$^{1–3}$ and **1**–**3** undergo cleavage of the *tert*-butylamide upon addition of $Me_4NOH\cdot 5H_2O$ (1 equiv.) in methanol at 50(1) °C. The rate of amide cleavage follows the order **1** > **2** ⩾ **3**, **L**$^{1–3}$. The extent by which the amide cleavage reaction is accelerated in **1**–**3** relative to the free ligands, **L**$^{1–3}$, is correlated with the strength of amide oxygen binding and Lewis acidity of the zinc(II) centre in **1**–**3** deduced from the X-ray, NMR and IR studies.

Introduction

Peptidases catalyze the hydrolysis of peptide bonds of polypeptides and proteins. These enzymes commonly require a single metal ion, typically zinc(II), as essential co-factor. Despite the considerable current interest in developing synthetic peptidases, the precise roles of the metal ions and the mechanisms of hydrolysis of peptide bonds in peptidases are not well understood.[1,2] Understanding the basic principles of peptide hydrolysis by peptidases, however, is necessary for the rational design of synthetic peptidases, for which important applications in biotechnology have been envisioned.[3]

In catalytic zinc sites such as those of peptidases, the zinc(II) ion is in a coordination environment in which three binding sites are taken by protein residues with a binding frequency of His ⩾ Glu >Asp = Cys.[4] The fourth or even additional sites can be occupied by water and/or the peptide substrate, and as a result, these sites are utilized for promoting amide hydrolysis. Although the mechanisms of metal-promoted amide hydrolysis are less certain than those of phosphate diester hydrolysis, it has been proposed that metal ions can promote the hydrolysis of peptide bonds in one of the following ways;[5] (1) by activating the carbonyl bond (electrophile activation); (2) by providing a nucleophile (OH) at neutral pH and (3) by providing a way to simultaneously activate the carbonyl bond and to generate the nucleophile at neutral pH (Scheme 1).

Several metal complexes have been used as synthetic models for peptidases. Substitutionally inert metal complexes of Co(III) have demonstrated that amide hydrolysis can be promoted both through activation of the carbonyl or intramolecular attack of a metal bound hydroxide.[6] In most of these studies, however, the simultaneous activation of nucleophile and electrophile species through metal coordination was not possible due to the nature of the complex formed. Moreover, only a few substitutionally labile model complexes of peptidases with biologically relevant metal ions such as Cu(II) and Zn(II) are known,[7] and as a result, there is even less mechanistic information available on labile metal-promoted amide hydrolysis.

In this report we investigate the use of the ligand unit (6-pivaloylamido-2-pyridylmethyl)amine as a way to induce an N_2O coordination environment for zinc(II) ions, in which oxygen coordination is provided by an intramolecular amide carbonyl group. This ligand moiety as part of three polydentate ligands with and without additional coordinating groups allows the formation of zinc(II) complexes with different coordination environments. The structures and amide oxygen binding strength of the three zinc(II) complexes in the solid state and in solution are compared. Amide cleavage reactions of these ligands and their zinc(II) complexes are investigated. Zinc(II)-promoted amide cleavage in methanol is observed in two of the complexes. The rate of amide cleavage appears to be correlated with the strength of amide coordination and Lewis acidity of the zinc(II) centre determined by X-ray, NMR and IR studies.

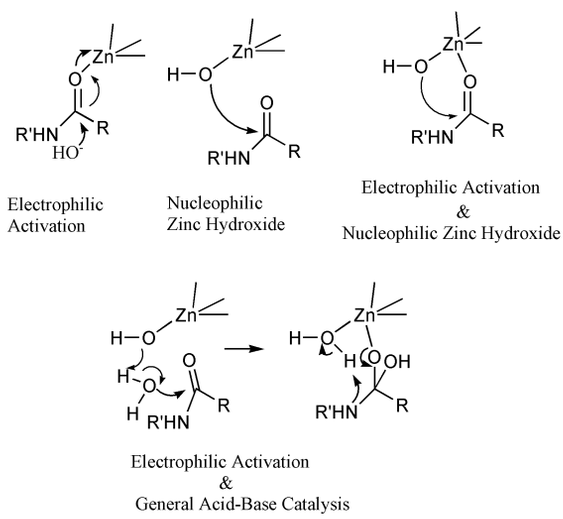

Scheme 1

Results and discussion

Design and synthesis

The ligand unit (6-pivaloylamido-2-pyridylmethyl)amine ideally positions an amide oxygen for intramolecular metal coordination. This fragment can be incorporated into a variety of polydendate ligands thus allowing the formation of metal complexes with different coordination environments and amide oxygen coordination as models for peptidases. In this work we show that ligands **L**^{1}, **L**^{2} and **L**^{3} provide N_4O, N_2S_2O and N_2O coordination for zinc when reacted with a suitable zinc precursor (Scheme 2).

DOI: 10.1039/b312221b

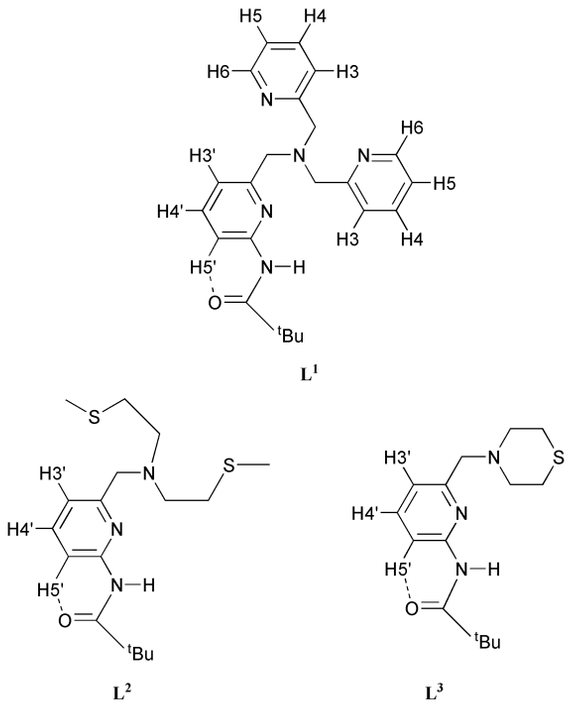

Scheme 2

The reaction of $\mathbf{L}^{1,3}$ with equimolar amounts of $ZnCl_2$ affords complexes which exhibit internal N–H ··· Cl–Zn hydrogen bonding.[8] The reaction of $\mathbf{L}^{1,2}$ with $[Zn(NCCH_3)_4](PF_6)_2$ or $Zn(ClO_4)_2{\cdot}6H_2O$, however, affords trigonal bipyramidal $[(\mathbf{L}^{1,2})Zn]^{2+}$ cations in which the carbonyl oxygen of the pivaloylamido group is coordinated axially.[8,9] Similarly, the reaction of equimolar amounts of $Zn(ClO_4)_2{\cdot}6H_2O$ and $\mathbf{L}^3$ affords a complex with amide oxygen coordination that, in addition, can accommodate a variety of additional ligands including water (Scheme 3). Thus, $\mathbf{L}^3$ allows the simultaneous coordination of an amide oxygen and a water molecule to a zinc(II) ion, a structural motif relevant to postulated mechanisms of zinc-promoted hydrolysis of peptide bonds in peptidases (Scheme 1).[1,2,5]

X-Ray crystallography

Structure of 3. Single crystals of **3** suitable for X-ray diffraction were grown by slow evaporation of acetonitrile solutions. A thermal ellipsoid plot of the molecular structure of **3** is shown in Fig. 1 and a list with selected distances and angles is given in Table 1. The zinc(II) centre is in a square pyramidal environment in which the base of the pyramid is formed by the pyridine and amine units, the amide oxygen and the water molecule. The acetonitrile molecule completes the pyramid by occupying the apical position. The square pyramidal geometry, however, is quite distorted (O(1W)–Zn–N(1S) 103.1(10)°, O(1W)–Zn–N(2) 151.17(9)°, N(2)–Zn–N(1S) 105.65(9)°) leaving a readily accessible coordination site adjacent to the amide oxygen, which in the crystal structure is weakly occupied by a ClO_4^- anion (O(3A) ··· C(8) 3.181(3) Å, Zn–O(3A) 2.955(3) Å, O(3A)–Zn–N(1S) 166.43(8)°, O(3A)–Zn–O(1W) 77.5(8)°). The Zn–O(8) distance, 2.0306(19) Å, is slightly longer than in **1**[8a] (2.0005(16) Å) and **2**[9] (2.006(3) Å). This structural feature suggests that the amide oxygen binds somewhat more weakly to the zinc(II) centre of **3** than to that of **1** or **2**. The angle N(1)–

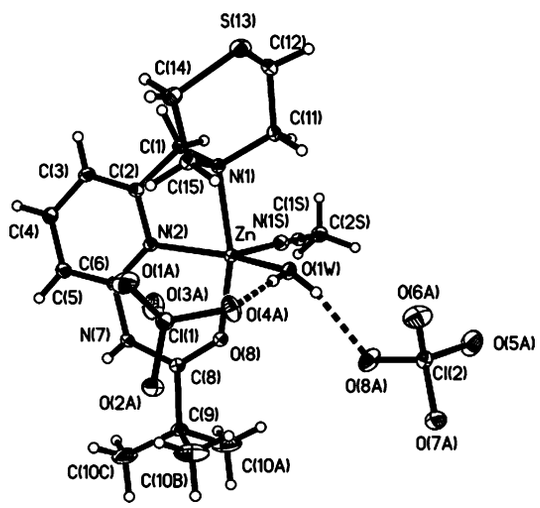

Fig. 1 Thermal ellipsoid plot drawn with 30% probability ellipsoids of the molecular structure of the $[(\mathbf{L}^3)Zn)(H_2O)(CH_3CN)](ClO_4)_2$ **3**.

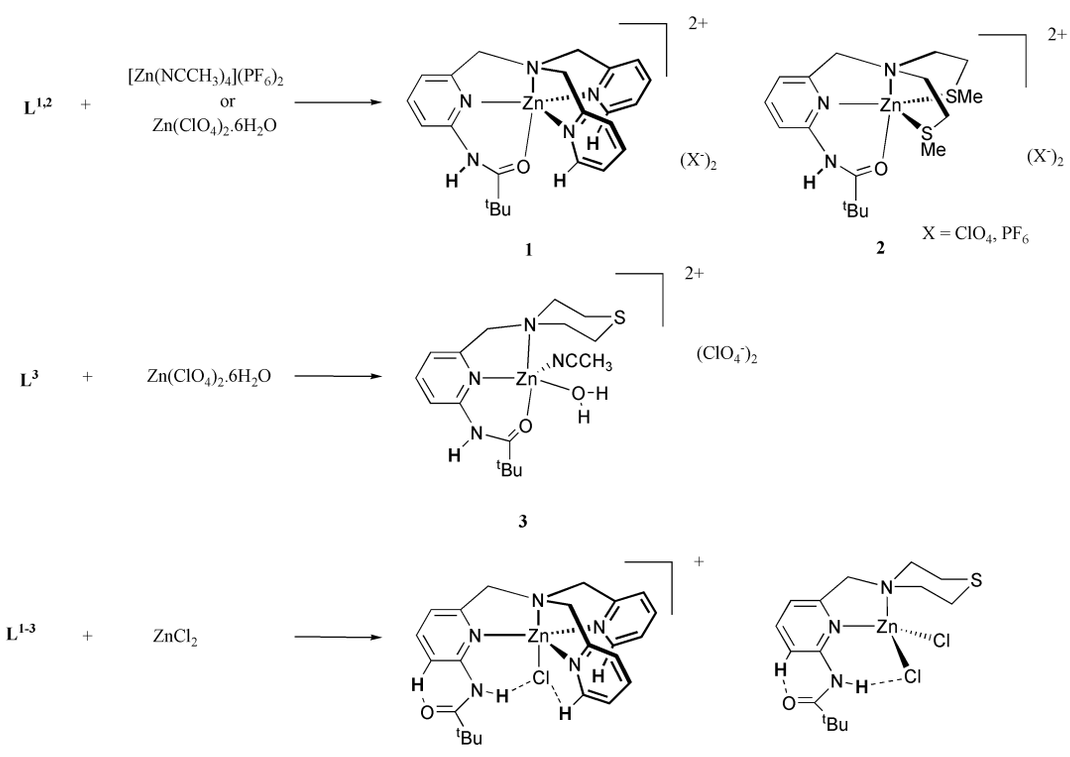

Scheme 3

Table 1 Selected bond lengths (Å) and angles (°) for **3**

Distances		Angles	
Zn–O(1W)	2.001(2)	O(1W)–Zn–N(1S)	103.1(10)
Zn–O(8)	2.0306(19)	O(1W)–Zn–N(2)	151.17(9)
Zn–N(1)	2.169(2)	N(2)–Zn–N(1S)	105.65(9)
Zn–N(2)	2.049(2)	O(1W)–Zn–O(8)	93.39(8)
Zn–N(1S)	2.056(2)	O(1W)–Zn–N(1)	92.67(8)
		O(8)–Zn–N(1S)	93.89(8)
N(7)–C(6)	1.402(3)	N(1S)–Zn–N(1)	98.79(9)
N(7)–C(8)	1.350(3)	N(2)–Zn–O(8)	86.91(8)
C(8)–O(8)	1.234(3)	N(2)–Zn–N(1)	80.85(8)
C(8)–C(9)	1.529(4)	O(8)–Zn–N(1)	164.33(8)
		C(8)–N(7)–C(6)	130.1(2)
		N(7)–C(8)–C(9)	117.5(2)
		O(8)–C(8)–N(7)	123.5(2)
		O(8)–C(8)–C(9)	119.0(2)

Table 2 Summary of selected ^{1}H NMR (360 MHz, CD_3CN, 293 K) chemical shift data for $\mathbf{L}^{1-3}$ and **1**–**3**[a]

		$\mathbf{L}^{1,2}$	**1**,**2**
^{t}Bu	H10	1.26, 1.26	1.55 (+0.29), 1.38 (+0.12)
NH	H7	8.16, 8.24	9.54 (+1.38), 9.39 (+1.15)
PyCH_2N	H1′$_{A,B}$	3.71, 3.68	4.33 (+0.62), 4.21 (+0.53)
Py (aromatic)	H3′	7.32, 7.24	7.39 (+0.07), 7.42 (+0.18)
	H4′	7.67, 7.70	8.10 (+0.43), 8.15 (+0.45)
	H5′	7.98, 8.00	7.51 (–0.53), 7.49 (–0.51)
		$\mathbf{L}^3$	**3**
^{t}Bu	H10	1.26	1.36 (+ 0.10)
NH	H7	8.26	9.32 (+1.06)
PyCH_2N	H1′$_{A,B}$	3.50	4.09 (+0.59)
Py (aromatic)	H3′	7.14	7.35 (+0.21)
	H4′	7.69	8.10 (+0.41)
	H5′	8.00	7.41 (–0.59)

[a] Chemical shifts are in ppm relative to CH_3CN at 1.94 ppm. Values in parentheses denote chemical shifts downfield (positive) or upfield (negative) *vs.* values in previous column. The symbol ′ refers to the 2-pyridylmethyl with the 6-pivaloylamido group.

Zn–O(8) of 164.33(8)° is smaller than in **1** (167.75(6)°) and **2** (167.5(2)°), *i.e.* it deviates even further from linearity. An important difference between the coordination environment of **3** compared to **1** or **2** is the simultaneous coordination of the amide oxygen and a water molecule (Zn–O(1W), 2.001(2) Å). The simultaneous binding of an amide oxygen and water molecule is a structural feature proposed for the double activation mechanism exerted by the Lewis acidic zinc(II) centre in peptidases and proteases. The zinc-bound water (O(1W)) is 4.041 Å away from the carbon of the amide group (C(8)) and doubly hydrogen bonded to the two ClO_4^- counter ions (O(1W) ··· O(4A) 2.700(3) Å, O(1W) ··· O(8A) 2.740(3) Å).

NMR and IR studies

Solution structures. Zinc(II) complexes **1**–**3** in acetonitrile solutions are all characterized by ^{1}H NMR resonances shifted downfield relative to the corresponding 'free' ligand ($\mathbf{L}^{1-3}$), a feature consistent with metal binding (Table 2, Fig. 2(a)). This downfield shift is more prominent for the amide N–H resonance, which is shifted by 1.38, 1.15 and 1.06 ppm in **1**, **2** and **3**, respectively, presumably a suggestion that the strength of amide oxygen coordination to the zinc(II) centre follows the order **1** > **2** > **3**. The feature of the ^{1}H NMR spectra of $\mathbf{L}^{1-3}$ and **1**–**3** that is most informative of the structure adopted, however, is the chemical shift of H5′, as it gives information of the orientation of the amide group. In $\mathbf{L}^{1-3}$ the H5′ resonance appears considerably downfield of the other aromatic resonances due to the close proximity of H5′ and the amide oxygen.[8] Thus, in **1**–**3** only the H5′ resonance undergoes a large upfield shift (0.55–0.59 ppm) relative to the corresponding ligand, something that is consistent with breaking a C–H5′ ··· O=C interaction, thus allowing amide oxygen binding to the zinc(II) centre. Very similar ^{1}H NMR spectra were obtained in methanol, which suggests that $\mathbf{L}^{1-3}$ and **1**–**3** adopt very similar structures in acetonitrile and methanol solutions (Fig. 2).

Table 3 Selected infrared and vibrational data of $\mathbf{L}^{1-3}$ and **1**–**3** in acetonitrile

	ν_{N-H}[a]/cm^{-1}	$\nu_{C=O}$[a]/cm^{-1}
$\mathbf{L}^1$	3439	1687
1	3320	1647
$\mathbf{L}^2$	3438	1683
2	3333	1642
$\mathbf{L}^3$	3439	1686
3	3361	1656

[a] ± 4 cm^{-1}.

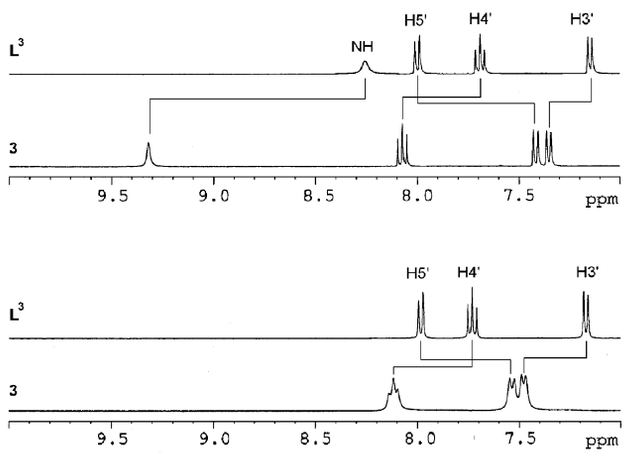

Fig. 2 Aromatic and NH region of the ^{1}H NMR (360.1 MHz, 293 K) of $\mathbf{L}^3$ (in CD_3CN), **3** (in CD_3CN), $\mathbf{L}^3$ (in CD_3OD) and **3** (in CD_3OD). See Table 3 for chemical shift values and Scheme 2 for labelling explanation.

^{13}C NMR studies provided an additional diagnostic parameter of the adopted structures and strength of amide oxygen binding in **1**–**3**. Thus, the position of the carbonyl resonances in the ^{13}C NMR spectra of **1**, **2** and **3** in acetonitrile of 187.1, 185.7 and 184.1 ppm, respectively, compared to 176.9 ppm for $\mathbf{L}^1$, 177.9 ppm for $\mathbf{L}^2$ and 177.9 ppm for $\mathbf{L}^3$ provides further evidence of carbonyl binding in **1**–**3**. The magnitude of the downfield shift experienced by the carbonyl resonance of 10.2 ppm for **1** relative to free $\mathbf{L}^1$, 7.8 ppm for **2** relative to $\mathbf{L}^2$ and 6.2 ppm for **3** relative to $\mathbf{L}^3$ reinforces that the strength of amide oxygen binding to the zinc(II) centre follows the order **1** > **2** > **3**.

IR studies are in total agreement with all the conclusions derived from the NMR and X-ray data regarding the strength of amide oxygen coordination to the zinc(II) centre in **1**–**3**. Thus, the IR spectra of **1**, **2** and **3** in acetonitrile show $\nu_{C=O}$ bands shifted to higher wavenumbers relative to the corresponding free ligand by 40 ± 4, 41 ± 4 and 30 ± 4 cm^{-1}, respectively (Table 3). The strength of amide oxygen coordination is also reflected in the extent by which the ν_{N-H} is shifted to lower wavenumbers, 119 ± 4 cm^{-1} for **1** relative to $\mathbf{L}^1$, 105 ± 4 cm^{-1} for **2** relative to $\mathbf{L}^2$ and 78 ± 4 cm^{-1} for **3** relative to $\mathbf{L}^3$. Both parameters are indicative of amide oxygen coordination being strongest in **1** and weakest in **3**.

Reactions with $Me_4NOH{\cdot}5H_2O$. Recently, it was reported that addition of $Me_4NOH{\cdot}5H_2O$ (1 equiv.) to **2** in methanol at 50(1) °C results in cleavage of the *tert*-butylamide to yield quantitatively the product of methanolysis methyl trimethylacetate.[9] It was also reported that under the same experimental

conditions $\mathbf{L}^2$ does not undergo amide cleavage after 140 h, which suggested that the amide methanolysis reaction was mediated by the zinc(II) ion. In an attempt to gain insights into the mechanism and chemical basis of why zinc(II) ions promote amide cleavage reactions we have compared the ability of $\mathbf{L}^{1–3}$ and **1**–**3** to undergo amide methanolysis. It was found that $\mathbf{L}^{1–3}$ and **1**–**3** all undergo amide cleavage in methanol upon addition of $Me_4NOH{\cdot}5H_2O$ (1 equiv.) at 50(1) °C (Figs. 3 and 4). In each case the reaction was monitored by ^{1}H NMR. After the addition of $Me_4NOH{\cdot}5H_2O$ the *tert*-butyl resonance of the amide appears at 1.47 ppm for **1**, 1.43 ppm for **2**, 1.37 ppm for **3** and 1.31 ppm for $\mathbf{L}^{1–3}$, which presumably reflects the different degrees of activation of the amide group for nucleophilic attack. Over time the amide resonance progressively disappears and a resonance at 1.18 ppm appears, which corresponds to methyl trimethylacetate (Fig. 4).[10] Given that the position of ^{1}H NMR resonance of the methyl trimethylacetate product is in all cases 1.18 ppm it is reasonable to suggest that this does not bind to the product zinc(II) complexes. In fact, over much longer periods of time, trimethylacetic acid is also formed at similar rates for **1**–**3** and $\mathbf{L}^{1–3}$, which is also consistent with the lack of binding of methyl trimethylacetate to a Zn^{2+} ion. Trimethylacetic acid, however, binds to the product zinc(II) complexes as judged by the position of the *tert*-butyl proton resonance, 1.39, 1.31, 1.25 and 1.13 ppm for **1**, **2**, **3** and $\mathbf{L}^{1–3}$, respectively. The half-life ($t_{1/2}$) of the amide bond was found to be 0.41 h for **1**, 3.95 h for **2**, 125 h for **3**, 55 h for $\mathbf{L}^1$, 60.1 h for $\mathbf{L}^2$ and 63.9 h for $\mathbf{L}^3$. Thus, amide cleavage of **1** *vs.* $\mathbf{L}^1$, **2** *vs.* $\mathbf{L}^2$ and **3** *vs.* $\mathbf{L}^3$ is accelerated by a factor of *ca.* 133, 15 and 0.5, respectively. The rate of amide cleavage correlates remarkably well with the X-ray, ^{1}H and ^{13}C NMR and IR data which suggested that the strength of the interaction between the zinc(II) centre and amide carbonyl group was **1** > **2** > **3**. Catalytic zinc sites possess a predominantly N-donating ligand[1] environment and only very rarely N/S ligation.[11–15] The rare occurrence of cysteine ligation in a few mononuclear and dinuclear catalytic zinc(II) active sites has prompted considerable research efforts toward the generation of zinc(II) complexes with mixed N/S coordination environments.[16] It is interesting to observe that the N_4 ligation of **1** is more efficient than the N_2S_2 coordination environment of **2** in promoting the amide cleavage reaction. The simultaneous binding of the amide group and water has been proposed as an event in one of the possible mechanisms of amide bond hydrolysis in metallopeptidases, which may be particularly efficient as it involves the zinc(II) centre bringing in close proximity and activating both nucleophile (water) and substrate (peptide) species. In **3**, however, despite the simultaneous amide/oxygen binding, amide cleavage is not accelerated relative to in the 'free' ligand, which is a significant finding.

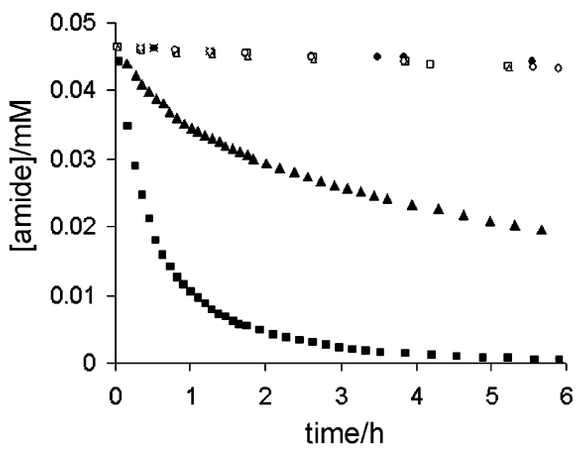

Fig. 3 Representative time courses for the reaction of **1** (■), **2** (▲), **3** (●), $\mathbf{L}^1$ (□), $\mathbf{L}^2$ (Δ) and $\mathbf{L}^3$ (○) (0.046 M) with $Me_4NOH{\cdot}5H_2O$ (1 equiv.) in methanol at 50 °C.

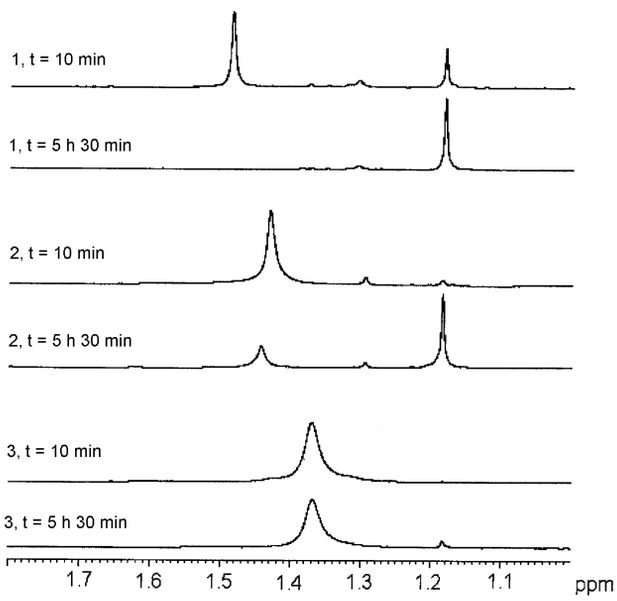

Fig. 4 ^{1}H NMR spectra of the reaction of **1**–**3** with $Me_4NOH{\cdot}5H_2O$ (1 equiv.) in d_4-MeOH at 50 °C showing in each case the resonance of the *tert*-butyl group of the starting amide (downfield signal) and the methyl trimethylacetate product (upfield signal) at t = 10 min and t = 5.5 h.

Conclusion

This study has explored fundamental chemical and structural features of zinc-mediated amide cleavage reactions. The approach consisted of using the ligand unit (6-pivaloylamido-2-pyridylmethyl)amine as a method to induce intramolecular amide oxygen coordination to a zinc(II) centre. The three ligands used, $\mathbf{L}^{1–3}$, formed mononuclear zinc(II) complexes with amide oxygen coordination to a zinc(II) centre with different coordination environments, **1**–**3**. The simultaneous binding of a water molecule and amide was observed in **3**. This arrangement resembles the motif that has been proposed to be involved in the double nucleophile/substrate Lewis acidic activation and positioning mechanism of amide bond hydrolysis in metallopeptidases.

A clear correlation was found between the information extracted from solid state and solution structural studies and that of functional studies. Thus, X-ray, ^{1}H and ^{13}C NMR and IR data suggest that the strength of amide oxygen binding follows the trend **1** > **2** > **3**, which would be consistent with the notion that the Lewis acidity of the zinc(II) centre follows the same order. We have found that **1**–**3** and $\mathbf{L}^{1–3}$ all undergo amide cleavage reactions in methanol upon addition of an equimolar amount of $Me_4NOH{\cdot}5H_2O$, and that the rate of the amide cleavage reaction follows the trend **1** > **2** > **3**, $\mathbf{L}^{1–3}$. Thus the observed trend in rate of amide methanolysis is identical to that of the strength of amide oxygen binding. Despite the simultaneous amide/water binding in **3**, its amide cleavage reaction is not accelerated relative to that of the free ligand $\mathbf{L}^3$. In contrast, this work showed that amide oxygen coordination is a key event in zinc-mediated amide cleavage reactions and that it is greatly influenced by the primary coordination sphere of the zinc(II) centre. From this work it appears that nitrogen is more efficient than mixed nitrogen/sulfur coordination, which would explain the binding frequency His ⩾ Glu > Asp = Cys found for catalytic zinc sites in Nature.

Experimental

General

Reagents were obtained from commercial sources and used as received unless otherwise noted. Solvents were dried and

purified under N_2 by using standard methods[17] and were distilled immediately before use. All compounds were prepared under N_2 unless otherwise mentioned. $\mathbf{L^1}$, $\mathbf{L^2}$, $\mathbf{L'^1}$, $\mathbf{L'^2}$ and **2** were synthesized according to recently reported procedures.[8,9] The NMR spectra were obtained using a Bruker DPX 360 at 20 °C in CD_3CN unless otherwise noted. ^{13}C and ^1H chemical shifts are referenced with respect to the carbon (δ_C 1.32 and 118.26 ppm) and residual proton (δ_H 1.94 ppm) solvent peaks. Peak assignments are done with the aid of 2-D NMR spectroscopy. Sample concentrations for the NMR studies were 0.02–0.04 M. Mass spectra were performed on a micromass Platform II system operating in Flow Injection Analysis mode with the electrospray method. Elemental analyses were carried out by the microanalyses service provided by the School of Chemistry at the University of Edinburgh. Infrared spectra were recorded with a JASCO FTIR-410 spectrometer between 4000 and 250 cm^{-1} as KBr pellets (solid state) or as acetonitrile solutions in KBr cells.

Synthesis

$\mathbf{L^3}$. Thiomorpholine (14.75 mmol, 1.5 cm^3) and Na_2CO_3 (145 mmol, 17.5 g) were dissolved in CH_3CN (~150 cm^3). This solution was then treated with 2-(pivaloylamido)-6-(bromomethyl)pyridine[18] (14.75 mmol, 4 g) and the resulting mixture was stirred for 24 h at 80 °C. The solution was cooled to room temperature, and then poured in 1 M $NaOH_{(aq)}$ (200 cm^3). The product was extracted with CH_2Cl_2 (3 × 150 cm^3). The organic phase was collected, dried over Na_2SO_4, and concentrated under reduced pressure to afford a yellow oil. This crude material was purified by flash chromatography (silica gel, EtOAc–hexanes (2 : 1)) to give the pure product (2.4 g, 55%) (Found: C, 61.61; H, 7.80; N, 14.27. for Calc. for $C_{15}H_{23}N_3OS$: C, 61.40; H, 7.90; N, 14.32%).

^1H NMR (CD_3CN, 360.1 MHz): δ_H 8.26 (br s, 1H, py′-N*H*), 8.00 (d, J = 8.3 Hz, 1H, py′-H5), 7.69 (t, J = 7.9 Hz, 1H, py′-H4), 7.14 (d, J = 7.3 Hz, 1H, py′-H3), 3.50 (s, 2H, NCH_2-py′), 2.70–2.60 (m, 8H, N(CH_2CH_2)$_2$S), 1.26 (s, 9H, C(CH_3)$_3$). ^{13}C NMR (CD_3CN, 90.5 MHz): δ_C 177.9 (C=O), 158.3 (py′-C2), 152.2 (py′-C6), 139.5 (py′-C3), 119.3 (py-C4′), 112.6 (py′-C5), 65.3 (N*C*H_2-py′), 55.8 and 28.5 (N(CH_2CH_2)$_2$S), 40.3 (*C*(CH_3)$_3$), 27.4 (C(*C*H_3)$_3$). ESI-MS (+ion): found m/z 294.2 (100%), calc. 294.16 (100%) for $[(\mathbf{L^3})H]^+$, and matches theoretical isotope distribution.

$\mathbf{L^{3'}}$. $\mathbf{L^3}$ (2.39 mmol, 0.7 g) was dissolved in 2 M HCl (50 cm^3). The resulting solution was heated at reflux overnight. The solution was allowed to cool to room temperature, after which, 1 M NaOH was added until pH ~13. The product was extracted with CH_2Cl_2 (3 × 100 cm^3). The combined organic phases were dried over Na_2SO_4 and evaporated to dryness under reduced pressure to afford the ligand as a yellow solid, which was recrystallised from diethyl ether (0.410 g, 82%) (Found: C, 57.19; H, 7.36; N, 18.85. Calc. for $C_{10}H_{15}N_3S{\cdot}0.14(CH_3CH_2)_2O$: C, 57.74; H, 7.53; N, 19.11%).

^1H NMR (CD_3CN, 360.1 MHz): δ_H 7.37 (t, J = 7.9 Hz, 1H, py′-H4), 6.64 (d, J = 7.2 Hz, 1H, py′-H3), 6.35 (d, J = 7.9 Hz, 1H, py′-H5), 4.8 (br, 2H, py′-N*H*$_2$), 3.40 (s, 2H, NCH_2-py′), 2.69–2.60 (m, 4H and 4H, N(CH_2CH_2)$_2$S). ^{13}C NMR (CD_3CN, 90.5 MHz): δ_C 159.9 and 157.9 (py′-C2 and py′-C6), 138.6 (py′-C3), 112.7 and 107.2 (py′-C4 and py′-C5), 65.7 (N*C*H_2-py′), 55.9 and 28.5 (N(CH_2CH_2)$_2$S). ESI-MS (+ion): found m/z 209.7 (100%), calc. 210.11 (100%) for $[(\mathbf{L^{3'}})H]^+$, and matches theoretical isotope distribution.

$[(\mathbf{L^1})Zn](ClO_4)_2$ 1. $Zn(ClO_4)_2{\cdot}6H_2O$ (94 mg, 0.25 mmol) and $\mathbf{L^1}$ (73 mg, 0.25 mmol) were dissolved in acetonitrile (5 cm^3) and the solution was stirred for 1 h at room temperature. The solution was filtered through Celite and the solvent evaporated under vacuum to yield the pure product as a yellow solid in quantitative yield (Found: C, 39.79; H, 4.19; N, 10.53. Calc. for $C_{23}H_{27}Cl_2N_5O_9Zn{\cdot}2H_2O$: C, 40.05; H, 4.53; N, 10.15%).

^1H NMR (CD_3CN, 360.1 MHz): δ_H 9.54 (br s, 1H, NH), 8.58 (d, J = 5.4 Hz, 2H, py-H6), 8.14 (td, J = 7.6, 1.5 Hz, 2H, py-H4), 8.10 (t, J = 7.9 Hz, 1H, py′-H4), 7.66 (t, J = 5.9 Hz, 2H, py-H5), 7.61 (d, J = 7.9 Hz, 2H, py-H3), 7.51 (d, J = 8.3 Hz, 1H, py′-H5), 7.39 (d, J = 7.6 Hz, 1H, py′-H3), 4.57 (s, 4H, NCH_2-py), 4.33 (s, 2H, NCH_2-py′), 1.55 (s, 9H, C(CH_3)$_3$). ^{13}C NMR (CD_3CN, 90.5 MHz, 298 K): δ_C 187.1 (C=O) 156.0 (py-C2) 153.6 and 152.4 (py′-C2 and py′-C6), 149.3 (py-C6), 144.5 (py′-C3), 142.9 (py-C3), 126.4 and 125.8 (py-C4 and py-C5), 122.1 and 115.1 (py′-C4 and py′-C5), 58.2 (N*C*H_2-py), 57.9 (N*C*H_2-py′), 42.6 (*C*(CH_3)$_3$), 27.1 (C(*C*H_3)$_3$). ESI-MS (+ion) found m/z 226.6 (100%), calc. 226.57 for $[(\mathbf{L^1})Zn]^{2+}$, and matches theoretical isotope distribution.

$[(\mathbf{L^3})Zn(H_2O)(CH_3CN)](ClO_4)_2$ 3. $Zn(ClO_4)_2{\cdot}6H_2O$ (149 mg, 0.4 mmol) and $\mathbf{L^3}$ (117 mg, 0.4 mmol) were dissolved in acetonitrile (15 cm^3) and the solution was stirred for 1 h at room temperature. The solvent was evaporated under vacuum to yield the pure product as a yellow solid in quantitative yield (Found: C, 32.69; H, 4.48; N, 8.84. Calc. for $C_{17}H_{28}Cl_2N_4O_{10}$-SZn: C, 33.10; H, 4.58; N, 9.08%).

^1H NMR (CD_3CN, 360.1 MHz): δ_H 9.32 (br s, 1H, NH), 8.10 (dd, J = 8.6, 7.9 Hz, 1H, py′-H4), 7.42 (d, J = 8.3 Hz, 1H, py′-H5), 7.35 (d, J = 7.6 Hz, 1H, py′-H3), 4.09 (s, 2H, NCH_2-py), 3.35–2.53 (m, 8H, N(CH_2CH_2)$_2$S) 1.37 (s, 9H, C(CH_3)$_3$). ^{13}C NMR (CD_3CN, 90.5 MHz, 298 K): δ_C 184.1 (C=O) 152.4 and 151.9 (py′-C2 and py′-C6), 143.9 (py′-C3), 121.8 and 116.7 (py′-C4 and py′-C5), 56.5 (N*C*H_2-py′), 54.7 and 22.1 (N(CH_2CH_2S)$_2$), 41.7 (*C*(CH_3)$_3$), 26.9 (C(*C*H_3)$_3$).

X-Ray crystallography

Crystal data for $[(\mathbf{L^3})Zn(OH_2)(NCCH_3)](ClO_4)_2$: $C_{17}H_{28}N_4O_{10}$-Cl_2SZn, M = 616.76, orthorhombic, space group *Pbca*, a = 17.5901(18), b = 15.6105(16), c = 18.4076(19), U = 5054.5(9) Å^3, Z = 8, T = 150(2) K, λ(Mo-Kα) = 0.71073, D_c = 1.621, μ = 1.324 mm^{-1}, 30143 reflections measured, 6288 unique, R_{int} = 0.0551 (all data), R_1 = 0.0628 (all data), wR_2 = 0.1299 (all data), S = 1.069 (all data), largest difference peak, hole 1.04, −0.65 e^- Å^{-3}.

Crystals suitable for X-ray diffraction studies were grown by slow evaporation of acetonitrile solutions at room temperature.

Intensity data for $[(\mathbf{L^3})Zn(OH_2)(NCCH_3)](ClO_4)_2$ were collected at 150 K using a Bruker (formerly Siemens) AXS SMART APEX area detector diffractometer with graphite-monochromated Mo-Kα radiation (λ = 0.71073 Å). The structures were solved by direct methods and refined to convergence against F^2 data using the SHELXTL suite of programs.[19] Data were corrected for absorption applying empirical methods using the program SADABS,[20] and the structures were checked for higher symmetry using the program PLATON.[21] All non-hydrogen atoms were refined anisotropically unless otherwise noted. Hydrogen atoms were placed in idealized positions and refined using a riding model with fixed isotropic displacement parameters. The N-H hydrogens were located in the difference map and refined isotropically.

CCDC reference number 220987.

See http://www.rsc.org/suppdata/dt/b3/b312221b/ for crystallographic data in CIF or other electronic format.

Acknowledgements

We gratefully acknowledge the EPSRC (GR/R25743/01), the Royal Society (RSRG: 22702), the Nuffield Foundation (NAL/00286/G) and The University of Edinburgh for funding.

References and notes

1 (*a*) W. N. Lipscomb and N. Sträter, *Chem. Rev.*, 1996, **96**, 2375; (*b*) E. L. Hegg and J. N. Burstyn, *Coord. Chem. Rev.*, 1998, **173**, 133.

2 (*a*) D. W. Christianson and W. N. Lipscomb, *Acc. Chem. Res.*, 1989, **22**, 62; (*b*) H. Kim and W. N. Lipscomb, *Biochemistry*, 1991, **30**, 8171.

3 (*a*) T. N. Parac and N. M. Kostic, *J. Am. Chem. Soc.*, 1996, **118**, 51; (*b*) T. M. Rana and C. F. Meares, *Proc. Natl. Acad. Sci. USA*, 1991, **88**, 10578; (*c*) T. M. Rana and C. F. Meares, *J. Am. Chem. Soc.*, 1991, **113**, 1859.

4 B. L. Valle and D. S. Auld, *Proc. Natl. Acad. Sci. USA*, 1990, **87**, 220.

5 L. M. Sayre, *J. Am. Chem. Soc.*, 1986, **108**, 1632.

6 (*a*) P. A. Sutton and D. A. Buckingham, *Acc. Chem. Res.*, 1987, **20**, 357; (*b*) J. T. Groves and L. A. Baron, *J. Am. Chem. Soc.*, 1989, **111**, 5442; (*c*) K. Takasaki, J. H. Kim, E. Rubin and J. Chin, *J. Am. Chem. Soc.*, 1993, **115**, 1157.

7 (*a*) J. T. Groves and R. J. Rife Chambers, Jr., *J. Am. Chem. Soc.*, 1984, **106**, 630; (*b*) T. H. Fife and T. J. Przystas, *J. Am. Chem. Soc.*, 1986, **108**, 4631; (*c*) L. M. Sayre, K. V. Reddy, A. R. Jacobson and W. Tang, *Inorg. Chem.*, 1992, **31**, 935; (*d*) J. Chin, V. Jubian and K. Mrejen, *J. Am. Chem. Soc.*, 1995, **117**, 7015; (*e*) E. L. Hegg and J. N. Burstyn, *J. Am. Chem. Soc.*, 1995, **117**, 7015; (*f*) X. S. Tan, Y. Fujii, T. Sato, Y. Nakano and M. Yashiro, *Chem. Commun.*, 1999, 881.

8 (*a*) J. C. Mareque Rivas, R. Torres Martín de Rosales and S. Parsons, *Dalton Trans.*, 2003, 2156; (*b*) J. C. Mareque Rivas, E. Salvagni, R. Torres Martín de Rosales and S. Parsons, *Dalton Trans.*, 2003, 3339.

9 L. M. Berreau, M. M. Makwska-Grzyska and A. M. Arif, *Inorg. Chem.*, 2000, **39**, 4390.

10 To confirm the identity of the product(s) of the amide cleavage reactions of $\mathbf{L}^{1-3}$ and **1**–**3**, the ^{1}H NMR spectra of the reaction mixtures were compared with those of methyl trimethylacetate (Aldrich) or trimethylacetic acid (Aldrich) added to an NMR tube containing the corresponding amino ligands 6-amino-2-pyridylmethyl)–R $\mathbf{L'}^{1-3}$ (R = bis(2-pyridylmethyl)amine $\mathbf{L'}^1$, bis(2-(methylthio)ethyl)amine $\mathbf{L'}^2$ and $N(CH_2CH_2)_2S$ $\mathbf{L'}^3$) (or equimolar amounts of $\mathbf{L'}^{1-3}$ and $Zn(ClO_4)_2{\cdot}6H_2O$) in CD_3OD (0.045 M).

11 H. Eklund and C.-I. Brändén, in *Zinc Enzymes*, ed. T. G. Spiro, John Wiley and Sons, New York, 1983, pp. 125–152.

12 M. K. Chan, W. Gong, P. T. R. Rajagopalan, B. Hao, C. M. Tsai and D. Pei, *Biochemistry*, 1997, **36**, 13904.

13 L. Betts, S. Wiang, S. A. Short, R. Wolfenden and C. W. Carter, Jr., *J. Mol. Biol.*, 1994, **235**, 635.

14 M. H. Bracey, J. Christiansen, P. Tovar, S. P. Cramer and S. G. Bartlett, *Biochemistry*, 1994, **33**, 12126.

15 Z. Wang, W. Fast, A. M. Valentine and S. J. Benkovic, *Curr. Opin. Chem. Biol.*, 1999, **3**, 614.

16 (*a*) L. M. Berreau, R. A. Allred, M. Makowska-Grzyska and A. M. Arif, *Chem. Commun.*, 2000, 1423, and references therein; (*b*) D. K. Garner, S. B. Fitch, L. H. McAlexander, L. M. Bezold, A. M. Arif and L. M. Berreau, *J. Am. Chem. Soc.*, 2002, **124**, 9970; (*c*) D. K. Garner, R. A. Allred, K. J. Tubbs and L. M. Berreau, *Inorg. Chem.*, 2002, **41**, 3533; (*d*) L. Berreau, M. M. Makowska-Grzyska and A. M. Arif, *Inorg. Chem.*, 2001, **40**, 2212.

17 W. L. F. Armarego and D. D. Perrin, *Purification of Laboratory Chemicals*, Butterworth-Heinemann, Oxford, 4th edn., 1997.

18 L. M. Berreau, S. Mahapatra, J. A. Halfen, V. G. Young, Jr. and W. B. Tolman, *Inorg. Chem.*, 1996, **35**, 6339.

19 SHELXS and SHELXL 97, G. M. Sheldrick, University of Göttingen, 1997.

20 (*a*) G.M. Sheldrick, SADABS, Empirical absorption correction program, University of Göttingen, 1995, based upon the method of Blessing; (*b*) R. H. Blessing, *Acta Crystallogr., Sect. A*, 1995, **51**, 33.

21 A. L. Spek, PLATON, *Acta Crystallogr., Sect. A.*, 1990, **46**, C–34.